Chapter 7
High-precision Modal Parameter Identification Algorithm Based on QR Decomposition

J. M. Liu and F. Liu

Abstract Modal parameters include modal frequency, damping ratio, modal shapes and participation factors. Traditional modal parameter identification algorithms do not yield the optimal result in least square sense, meaning that the error between the synthesized frequency response function (FRF) and measured FRF is not the least. By optimizing the identified modal parameters, theoretically, the unique modal parameters with the highest fitting accuracy can be obtained despite different modal parameter identification algorithm is used. When the number of modal parameters is large, optimizing all the modes simultaneously requires solving extremely large-scale linear equations, which is time-consuming and impractical in engineering applications. The algorithm proposed in this paper concentrates the parameters of modal frequency, damping ratio and participation factors in the latter part of the optimization equation through QR decomposition. This approach allows for considering all variables during each optimization, only calculating the optimized frequency, damping ratio and participation factors, without needing to solve extremely large-scale linear equations. The optimized modal shapes can be extracted point by point using linear equations from single measurement points' FRF or half power spectra. The proposed algorithm significantly improves computational speed, enabling the rapid acquisition of experimental modal parameters with the highest fitting accuracy.

Keywords Modal testing · High-precision · Modal parameter identification · QR decomposition · Optimization

Introduction

Modal testing is divided Experimental Modal Analysis(EMA) with measurable excitation force and Operational Modal Analysis(OMA) with unmeasurable excitation force. The modal parameters of EMA can be identified by FRF (Frequency domain) or impulse response function (Time domain), while in OMA, it is obtained by half power spectrum (Frequency domain) or by cross-correlation coefficients with positive time delay (Time domain). To identify close modes or to obtain accurate modal shapes for all orders, Multi-Input and Multi-Output (MIMO) experimental methods are often used. There are two types of MIMO in EMA, the first involves multiple excitations (the number of excitation points is equal to the number of reference points), measuring all responses; the second involves multiple fixed responses (the number of response points is equal to the number of reference points), exciting all measurement points. MIMO in OMA involves selecting multiple reference points. Sensors in these reference points should keep in the same position if the number of sensor is not enough to measure all points at one time.

The commonly used parameter identification algorithms in EMA include Eigensystem Realization Algorithm (ERA)[1], the PolyMAX[3] algorithm in frequency domain and the PolyIIR[4] algorithm in time domain Based on the Unified Matrix Polynomial Approach(UMPA)[2]. The commonly used parameter identification algorithms in OMA include Data-Driven Stochastic Subspace Identification (Data_Driver SSI)[5] based on the original data, the SSI(COV)[6] algorithm based on the half-spectrum, the Enhanced Frequency Decomposition (EFDD)[7]algorithm.as well as the PloyMAX algorithm in the frequency domain and the PolyIIR algorithm in the time domain based UMPA. All these algorithms except EFDD require the calculation of a stabilization graph, manual or automatic selection of physical poles to avoid mathematical poles, and

J.M.Liu · F. Liu
China Orient Institute of Noise & Vibration, Beijing 100085, China
e-mail: liujm@coinv.com; liuf@coinv.com

© The Author(s), under exclusive license to River Publishers 2026

Kristin B. Zimmerman, PhD (eds.), *Topics in Modal Analysis & Parameter Identification in Structural Dynamics, 2026, Vol. 8*,
Conference Proceedings of the Society for Experimental Mechanics Series, https://doi.org/10.13052/rp-9788743814191

then to extract the modal shapes of each mode. The obtained modal parameters are not the optimal result in least square sense, meaning that the error between the measured and synthesized FRF(EMA) or half spectrum (OMA) is not in the least.

By optimizing the modal parameters base on the initial result of different algorithms, the best result in least square sense can be obtained. In this way, the result of different algorithms can be unified, the precision of parameters will be greatly improved[8].

Modal parameters include poles (modal frequency and modal damping ratio), with a quantity of twice the total number of modes (including conjugate modes); modal participators, with a quantity of twice the total number of modes multiplied by the number of reference points; and modal shapes, with a quantity of twice the total number of modes multiplied by the number of measurement points.

Optimization algorithms can be divided into three types.

1. Fix modal shapes and participators, optimize to obtain new modal poles. Caculate the participators base on the new poles. Extract modal shapes point by point. Then, proceed to the next optimization cycle. This method can be realized very easily, but the efficiency of optimization is very low and cannot reach the optimal result, often stop at the initial result.
2. fix the modal shapes, optimize to obtain modal participators and the new poles. extract new modal shapes point by point. Then, proceed to the next optimization cycle. This method is easier to implement the algorithm 1 can be realized easily, optimization efficiency is better than method 1, but still can't reach the optimal solution.
3. Optimize all modal parameters simultaneously to obtain the optimized participators, poles and modal shapes. This algorithm can obtain the optimal solution. However, when the product of modal measurement points and the total number of modal order is large, solving extremely large-scale linear equations is required, which is very time consuming, making it impractical.

The algorithm proposed in the paper improves algorithm 3 by optimizing all modal parameters simultaneously. It concentrates the modal poles and participator in the latter part of the optimization equation, performs QR decompose on the linear equations, and firs solves for the optimized modal poles. Then, for each reference points, the optimized modal poles are used to establish equations containing participators and modal shapes, and QR decomposition is performed again to separately obtain the participator corresponding to each reference point. After obtaining the optimized modal poles and participator, the optimized modal shapes can be extracted point by point. Then, proceed to the next optimization cycle. By avoiding solve large dimension linear equations, This approach can significantly improve the computational speed.

Theory

The optimization algorithm has a premise, which is that the current solution is close to the optimal state and all parameters change slightly during the optimization process. Therefore, it is required that the initial solution obtained through the stability diagram includes all physical modal poles without missing any modes.

QR optimization algorithm for modal parameters

For MIMO modal parameters with normalized mass, assuming the number of exciting point is$p$, responding point is q, mode orders is$n$, and the initial solution of the modes is known. For responding point$i$, exciting point(or reference point)j, the theoretical function of FRF(EMA Test)or Half spectrum(OMA Test) is

$$\hat{H}_{ij}(s) = \frac{a_{ij}}{s} + b_{ij} + \sum_{r=1}^{2n} \frac{\phi_r^i L_r^j}{s - s_r} \tag{1}$$

Where the first term of right side of equation (1) is the low frequency garbage term, which can be seen as the influence of 0Hz, $a_{ij}$is a real number; the second term is the high frequency garbage term, which can be seen as the influence of$+\infty$.$b_{ij}$is a real number. ϕ_r^i,L_r^j and s_r are complex numbers, $\phi_r^i$is the modal shape of point $i$and mode order$r$,L_r^j is the participator of reference point $j$and mode order r,s_r is the pole of mode order$r$. There are n orders as well as corresponding conjugate orders. For OMA test, if test is measured by multiple groups, L_r^j is different in each group. To extract vibration shape, need to compute by group.

Taking the derivative of equation (1), we get:

$$H_{ij}(s) - \hat{H}_{ij}(s) = \frac{\Delta a_{ij}}{s} + \Delta b_{ij} + \sum_{r=1}^{2n} \frac{L_r^j}{s - s_r} \Delta \phi_r^i + \sum_{r=1}^{2n} \frac{\phi_r^i}{s - s_r} \Delta L_r^j + \sum_{r=1}^{2n} \frac{\phi_r^i L_r^j}{(s - s_r)^2} \Delta s_r \tag{2}$$

Where $H_{ij}(s)$ is obtained from actual measurements.
Define:

$$\sigma_r^j(s) = \frac{L_r^j}{s - s_r} \tag{3}$$

$$\psi_r^i(s) = \frac{\phi_r^i}{s - s_r} \tag{4}$$

Then we have

$$\begin{bmatrix} \frac{1}{s} & 1 & A_j & B_i & C_{ij} \end{bmatrix} \begin{bmatrix} \Delta a_{ij} \\ \Delta b_{ij} \\ \Delta \hat{\phi}_i \\ \Delta \hat{L}_j \\ \Delta \hat{\mathrm{s}} \end{bmatrix} = [\Delta H_{ij}(s)] \tag{5}$$

$$A_j = \begin{bmatrix} \sigma_1^j(s) & \sigma_2^j(s) & \cdots & \sigma_{2n}^j(s) \end{bmatrix} \tag{6}$$

$$B_i = \begin{bmatrix} \psi_1^i(s) & \psi_2^i(s) & \cdots & \psi_{2n}^i(s) \end{bmatrix} \tag{7}$$

$$C_{ij} = \begin{bmatrix} \psi_1^i(s)\sigma_1^j(s) & \psi_2^i(s)\sigma_2^j(s) & \cdots & \psi_{2n}^i(s)\sigma_{2n}^j(s) \end{bmatrix} \tag{8}$$

$$\Delta \hat{\phi}_i = \begin{bmatrix} \Delta \phi_1^i \\ \Delta \phi_2^i \\ \vdots \\ \Delta \phi_{2\mathrm{n}}^i \end{bmatrix} \tag{9}$$

$$\Delta \hat{L}_j = \begin{bmatrix} \Delta L_1^j \\ \Delta L_2^j \\ \vdots \\ \Delta L_{2\mathrm{n}}^j \end{bmatrix} \tag{10}$$

$$\Delta \hat{s} = \begin{bmatrix} \Delta s_1 \\ \Delta s_2 \\ \vdots \\ \Delta s_{2n} \end{bmatrix} \tag{11}$$

Equation (5) can be written in the form of a real coefficient equation as:

$$\begin{bmatrix} 0 & 1 & A1_j^{re} & -A2_j^{im} & B1_i^{re} & -B2_i^{im} & C1_{ij}^{re} & -C2_{ij}^{im} \\ \frac{-1}{\omega} & 0 & A1_j^{im} & A2_j^{re} & B1_i^{im} & B2_i^{re} & C1_{ij}^{im} & C2_{ij}^{re} \end{bmatrix} \begin{bmatrix} \Delta a_{ij} \\ \Delta b_{ij} \\ \Delta \hat{\phi}_i^{re} \\ \Delta \hat{\phi}_i^{im} \\ \Delta \hat{L}_j^{re} \\ \Delta \hat{L}_j^{im} \\ \Delta \hat{s}^{re} \\ \Delta \hat{s}^{im} \end{bmatrix} = \begin{bmatrix} \Delta H_{ij}^{re}(j\omega) \\ \Delta H_{ij}^{im}(j\omega) \end{bmatrix} \tag{12}$$

For n modes, their poles, participators and modal shapes all appear in conjugate forms. Equation (12) can be simplified to solve for the optimization parameters of modes by making slight adjustments to the matrix in equation (12).

$$A1_j^{re} = \begin{bmatrix} rea_1^j(s) & rea_2^j(s) & \cdots & rea_n^j(s) \end{bmatrix},$$

Where $rea_{\mathrm{r}}^{j}(s)$ is the real part of $\frac{L_r^j}{s-s_r}+\frac{(L_r^j)^*}{s-s_r^*}$

$$A1_j^{im}=\left[\begin{array}{cccc} ima_1^j(s) & ima_2^j(s) & \cdots & ima_n^j(s) \end{array}\right],$$

Where $\mathrm{i}ma_{\mathrm{r}}^{j}(s)$ is the imaginary part of $\frac{L_r^j}{s-s_r}+\frac{(L_r^j)^*}{s-s_r^*}$

$$B1_i^{re}=\left[\begin{array}{cccc} reb_1^i(s) & reb_2^i(s) & \cdots & reb_n^j(s) \end{array}\right],$$

Where $reb_{\mathrm{r}}^{i}(s)$ is the real part of $\frac{\phi_r^i}{s-s_r}+\frac{(\phi_r^i)^*}{s-s_r^*}$

$$B1_i^{im}=\left[\begin{array}{cccc} imb_1^i(s) & imb_2^i(s) & \cdots & imb_n^i(s) \end{array}\right],$$

Where $imb_{\mathrm{r}}^{j}(s)$ is the imaginary part of $\frac{\phi_r^i}{s-s_r}+\frac{(\phi_r^i)^*}{s-s_r^*}$

$$C1_{ij}^{re}=\left[\begin{array}{cccc} rec_1^{ij}(s) & rec_2^{ij}(s) & \cdots & rec_n^{ij}(s) \end{array}\right],$$

Where $rec_{\mathrm{r}}^{ij}(s)$ is the real part of $\frac{\phi_r^i L_r^j}{(s-s_r)^2}+\frac{(\phi_r^i)^*(L_r^j)^*}{(s-s_r^*)^2}$

$$C1_{ij}^{im}=\left[\begin{array}{cccc} imc_1^{ij}(s) & imc_2^{ij}(s) & \cdots & imc_n^{ij}(s) \end{array}\right],$$

Where $imc_{\mathrm{r}}^{ij}(s)$ is the imaginary part of $\frac{\phi_r^i L_r^j}{(s-s_r)^2}+\frac{(\phi_r^i)^*(L_r^j)^*}{(s-s_r^*)^2}$

Each element of $A2_j^{re}$ is the real part of $\frac{L_r^j}{s-s_r}-\frac{(L_r^j)^*}{s-s_r^*}$. The other matrix with 2 is similar, the operation sign from "+" change to "-".

Equation (12) simplify as

$$[X(j\omega)]_{2\times(2+6n)}\,\theta_{(2+6n)\times 1}=[Y(j\omega)]_{2\times 1} \tag{13}$$

Equation (13) holds for spectral lines of N, Equation (13) is expanded to

$$\left[\begin{array}{c} X(j\omega_1) \\ X(j\omega_2) \\ \vdots \\ X(j\omega_N) \end{array}\right]_{2N\times(2+6n)} \theta_{(2+6n)\times 1}=\left[\begin{array}{c} Y(j\omega_1) \\ Y(j\omega_2) \\ \vdots \\ Y(j\omega_N) \end{array}\right]_{2N\times 1} \tag{14}$$

Perform QR decomposition on the coefficient matrix of the left side of equation (14), we get:

$$\left[\begin{array}{c} X(j\omega_1) \\ X(j\omega_2) \\ \vdots \\ X(j\omega_N) \end{array}\right]=[Q_{ij}]_{2N\times 2N}\left[\begin{array}{cc} R_{11}^{ij} & R_{12}^{ij} \\ 0 & R_{22}^{ij} \\ 0 & 0 \end{array}\right]_{2N\times(2+6n)} \tag{15}$$

The decomposition R is illustrated in figure 1

Dimension of $[R_{22}^{ij}]$ is$2n\times 2n$, $[R_{11}^{ij}]$ is $(2+4n)\times(2+4n)$, $[R_{12}^{ij}]$ is $(2+4n)\times 2n$

Substitute (15) into (14) to obtain:

$$\left[\begin{array}{cc} R_{11}^{ij} & R_{12}^{ij} \\ 0 & R_{22}^{ij} \\ 0 & 0 \end{array}\right]\left[\begin{array}{c} \vdots \\ \Delta\hat{s}^{re} \\ \Delta\hat{s}^{im} \end{array}\right]=[Q_{ij}]^T\left[\begin{array}{c} Y(j\omega_1) \\ Y(j\omega_2) \\ \vdots \\ Y(j\omega_N) \end{array}\right]=\left[\begin{array}{c} S_{ij} \\ P_{ij} \\ T_{ij} \end{array}\right] \tag{16}$$

We can get:

$$[R_{22}^{ij}]\left[\begin{array}{c} \Delta\hat{s}^{re} \\ \Delta\hat{s}^{im} \end{array}\right]=P_{ij} \tag{17}$$

P_{ij} is the row of $3+4n$ to $2+6n$ in equation (16).

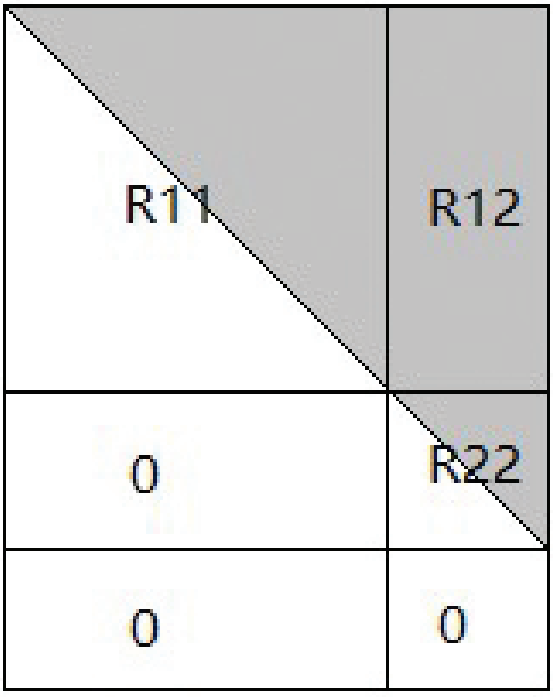


Fig. 1 QR decomposition illustration

Each excitation point(reference point) corresponds to q FRF or half spectrum curves for all response points. There are p excitation points, equation (17) is expanded to:

$$\begin{bmatrix} R_{22}^{11} \\ R_{22}^{21} \\ \vdots \\ R_{22}^{qp} \end{bmatrix}_{2pqn\times 2n} \begin{bmatrix} \Delta\hat{s}^{re} \\ \Delta\hat{s}^{im} \end{bmatrix} = \begin{bmatrix} P_{11} \\ P_{21} \\ \vdots \\ P_{qp} \end{bmatrix} \tag{18}$$

Thus

$$\left(\sum_{i=1}^{q}\sum_{j=1}^{p}\left[R_{22}^{ij}\right]^T\left[R_{22}^{ij}\right]\right)\begin{bmatrix} \Delta\hat{s}^{re} \\ \Delta\hat{s}^{im} \end{bmatrix} = \sum_{i=1}^{q}\sum_{j=1}^{p}\left[R_{22}^{ij}\right]^T[P_{ij}] \tag{19}$$

The least squares solution of the pole correction amount can be obtained from equation (19). After the pole correction is known, the calculation of the modal participator correction amount requires all curves corresponding to the same exciting point.

From equation (2), get

$$\frac{\Delta a_{ij}}{s} + \Delta b_{ij} + \sum_{r=1}^{2n}\frac{L_r^j}{s-s_r}\Delta\phi_r^i + \sum_{r=1}^{2n}\frac{\phi_r^i}{s-s_r}\Delta L_r^j = H_{ij}(s) - \hat{H}_{ij}(s) - \sum_{r=1}^{2n}\frac{\phi_r^i L_r^j}{(s-s_r)^2}\Delta s_r \tag{20}$$

(12) is rewritten as

$$\begin{bmatrix} 0 & 1 & A_j^{re} & -A_j^{im} & B_i^{re} & -B_i^{im} \\ \frac{-1}{\omega} & 0 & A_j^{im} & A_j^{re} & B_i^{im} & B_i^{re} \end{bmatrix}\begin{bmatrix} \Delta a_{ij} \\ \Delta b_{ij} \\ \Delta\hat{\phi}_i^{re} \\ \Delta\hat{\phi}_i^{im} \\ \Delta\hat{L}_j^{re} \\ \Delta\hat{L}_j^{im} \end{bmatrix} = \begin{bmatrix} J_{ij}^{re}(j\omega) \\ J_{ij}^{im}(j\omega) \end{bmatrix} \tag{21}$$

Simplify as

$$[V(j\omega)]_{2\times(2+4n)}\,\theta_{(2+4n)\times 1} = [J(j\omega)]_{2\times 1} \tag{22}$$

Equation (22) holds for spectral lines of N, equation (22) is expanded to:

$$\begin{bmatrix} V(j\omega_1) \\ V(j\omega_2) \\ \vdots \\ V(j\omega_N) \end{bmatrix}_{2N\times(2+4n)} \theta_{(2+4n)\times 1} = \begin{bmatrix} J(j\omega_1) \\ J(j\omega_2) \\ \vdots \\ J(j\omega_N) \end{bmatrix}_{2N\times 1} \tag{23}$$

Perform QR decomposition on the coefficient matrix of the left side of equation (23) to obtain:

$$\begin{bmatrix} V(j\omega_1) \\ V(j\omega_2) \\ \vdots \\ V(j\omega_N) \end{bmatrix} = [Q_{ij}]_{2N\times 2N} \begin{bmatrix} R_{11}^{ij} & R_{12}^{ij} \\ 0 & R_{22}^{ij} \\ 0 & 0 \end{bmatrix}_{2N\times(2+4n)} \tag{24}$$

The dimension of $[R_{22}^{ij}]$ is $2n \times 2n$, $[R_{11}^{ij}]$ is $(2+2n)\times(2+2n)$, $[R_{12}^{ij}]$ is $(2+2n)\times 2n$
Substitute into (23) to obtain:

$$\begin{bmatrix} R_{11}^{ij} & R_{12}^{ij} \\ 0 & R_{22}^{ij} \\ 0 & 0 \end{bmatrix} \begin{bmatrix} \vdots \\ \Delta\hat{L}_j^{re} \\ \Delta\hat{L}_j^{re} \end{bmatrix} = [Q_{ij}]^T \begin{bmatrix} J(j\omega_1) \\ J(j\omega_2) \\ \vdots \\ J(j\omega_N) \end{bmatrix} = \begin{bmatrix} S_{ij} \\ P_{ij} \\ T_{ij} \end{bmatrix} \tag{25}$$

We can get:

$$[R_{22}^{ij}] \begin{bmatrix} \Delta\hat{L}_j^{re} \\ \Delta\hat{L}_j^{re} \end{bmatrix} = P_{ij} \tag{26}$$

P_{ij} is the row of $3+2n$ to $2+4n$ in equation (25)
For each exciting point, there are q curves, equation (24) is expanded to:

$$\begin{bmatrix} R_{22}^{1j} \\ R_{22}^{2j} \\ \vdots \\ R_{22}^{qj} \end{bmatrix}_{2qn\times 2n} \begin{bmatrix} \Delta\hat{L}_j^{re} \\ \Delta\hat{L}_j^{re} \end{bmatrix} = \begin{bmatrix} P_{1j} \\ P_{2j} \\ \vdots \\ P_{qj} \end{bmatrix} \tag{27}$$

Therefore, we have

$$\left(\sum_{i=1}^{q} \left[R_{22}^{ij}\right]^T \left[R_{22}^{ij}\right]\right) \begin{bmatrix} \Delta\hat{L}_j^{re} \\ \Delta\hat{L}_j^{re} \end{bmatrix} = \sum_{i=1}^{q} \left[R_{22}^{ij}\right]^T [P_{ij}] \tag{28}$$

The least squares solution of the participator correction amount for the excitation point j can be obtained from equation (28).

After obtaining the optimized modal frequencies, damping ratios and participators, modal shapes can be extracted point by point, considering the influence of high frequency and low frequency garbage responses.

Finally, the optimization algorithm of parameters of MIMO modal test is surmised as bellow:

1. In each optimization process, modal frequencies, damping ratios, participators and modal shape should be optimized at the same time. The influence of low and high frequency garbage terms need to be considered.
2. To obtain the correction amount of modal frequencies and damping ratios, all curves should be considered. A single spectral line equation is constructed according to equation (12),and multiple spectral line equations are constructed through equation (14). After QR decomposition, we get the R matrix illustrated as figure 1, from which we can obtain equation (17) containing only the modal pole correction amount. Considering all curves, equation (18) is obtained, the optimized poles will be get in least square meaning.

3. To obtain the correction amount of modal participators, all curves corresponding to same excitation point are required. Equation (23) is obtained from equation (22), and equation (25) is obtained from the same excitation point corresponding to all response point curves. Equation (27) is extended using all response point curves, and the least squares method is used to obtain the correction amount of the participator.
4. Extract modal shapes point by point, considering the influence of low and high frequency garbage terms.
5. Caculate the fitting error coefficient to decide whether to continue the next loop of optimization.

Application

A MIMO test of a car brake disc was conducted to verify the optimization algorithm. The brake disc is shown as figure 2.

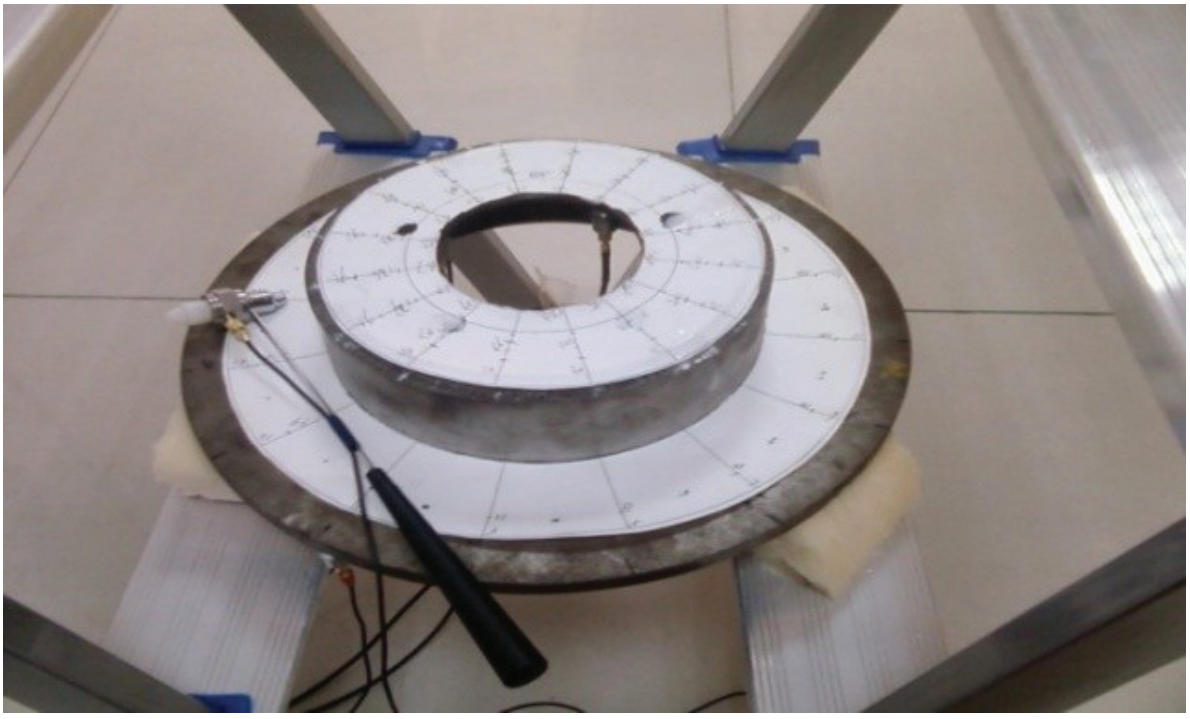


Fig. 2 The break disc of a car

The size of the break disc is as follows:

Outside diameter: R = 15cm, Inside diameter: R = 9cm, Innermost inner diameter R = 4cm, Height: 6cm, Bottom thickness: 1cm, Wall thickness: 0.7cm, Top thickness: 0.5cm. There are 5 evenly spaced small holes and one small hole near the edge on the top. Its mass is 5.18 kg.

A total of 160 measurement points were set, and four piezoelectric accelerometer weighing 8 grams were placed at point 1,7,15 and 22. By moving the excitation point with a hammer. 4 groups of FRFs with 8193 spectral lines are obtained for MIMO modal analysis. The analysis frequency is 6400Hz.

The initial solution was obtained by PolyIIR algorithm, with a total of 32 orders. The last two modes are used to ensure the stability and convergence of the optimization calculation process within the entire frequency band.

Three algorithms were used for Optimization. Algorithm 1 can't proceed, the initial result is the best result. Algorithm 2 reached the optimal result after 7 optimizations. Algorithm 3 can be optimized hundreds of times, but its optimization efficiency decreases evidently. The first 19 optimization data were taken to compare with algorithm 2. The optimization efficiency of different algorithm is illustrated in figure 3.

In the figure 3, the fitting error is the ratio of total root of mean square of error spectrum to measured spectrum.

The result of first loop of algorithm 3 is near the optimal result of algorithm 2, the result of second loop of algorithm 3 is better than the optimal result of algorithm 2.

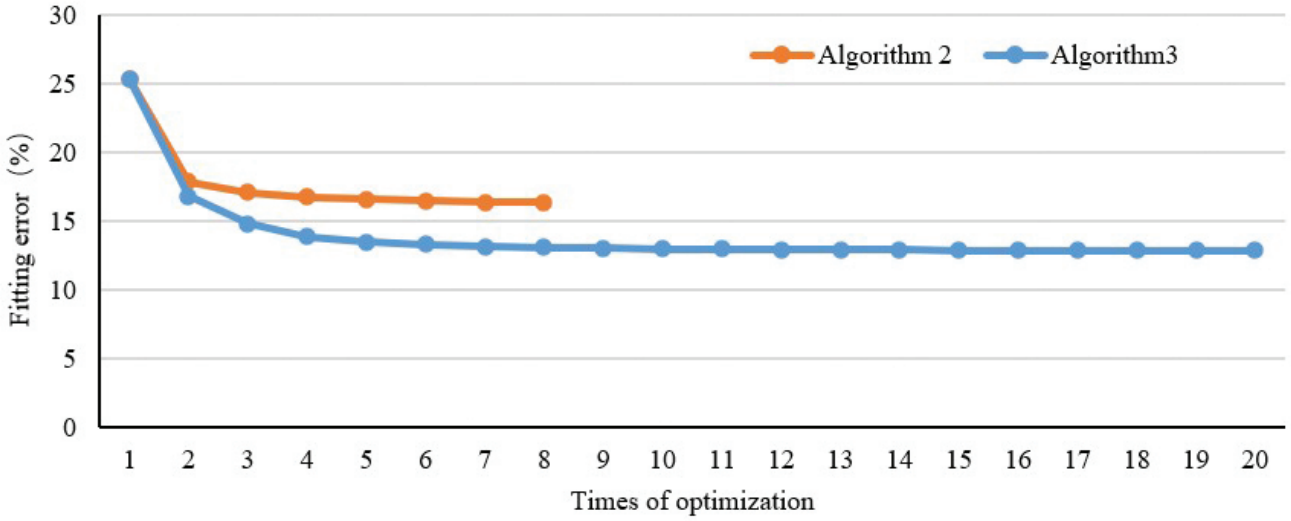


Fig. 3 Optimization efficiency of different algorithm

The foremost 30 modal shapes before optimization are illustrated in figure 4. The modal shapes after optimization by algorithm 2 are shown in figure 5. The modal shapes after optimization by algorithm 3 are shown in figure 6.

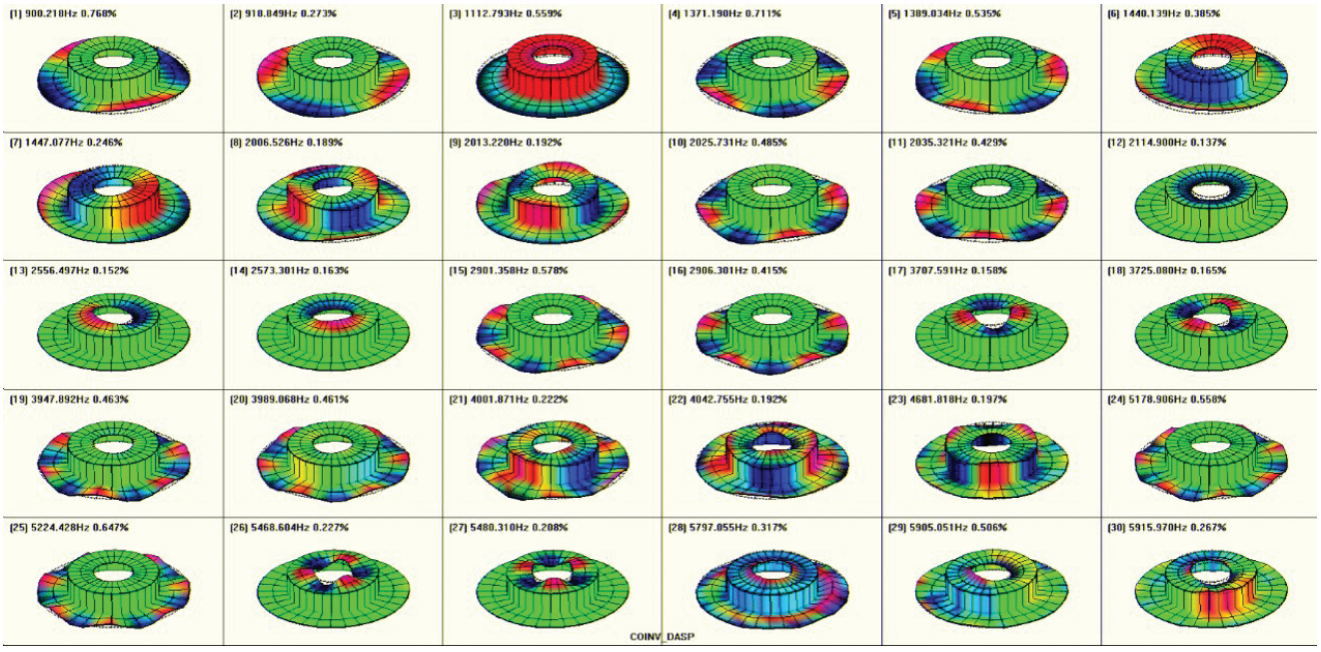


Fig. 4 Modal shapes before optimization

The modal frequencies, damping ratios and fitting errors before optimization and after optimization are listed in table 1.

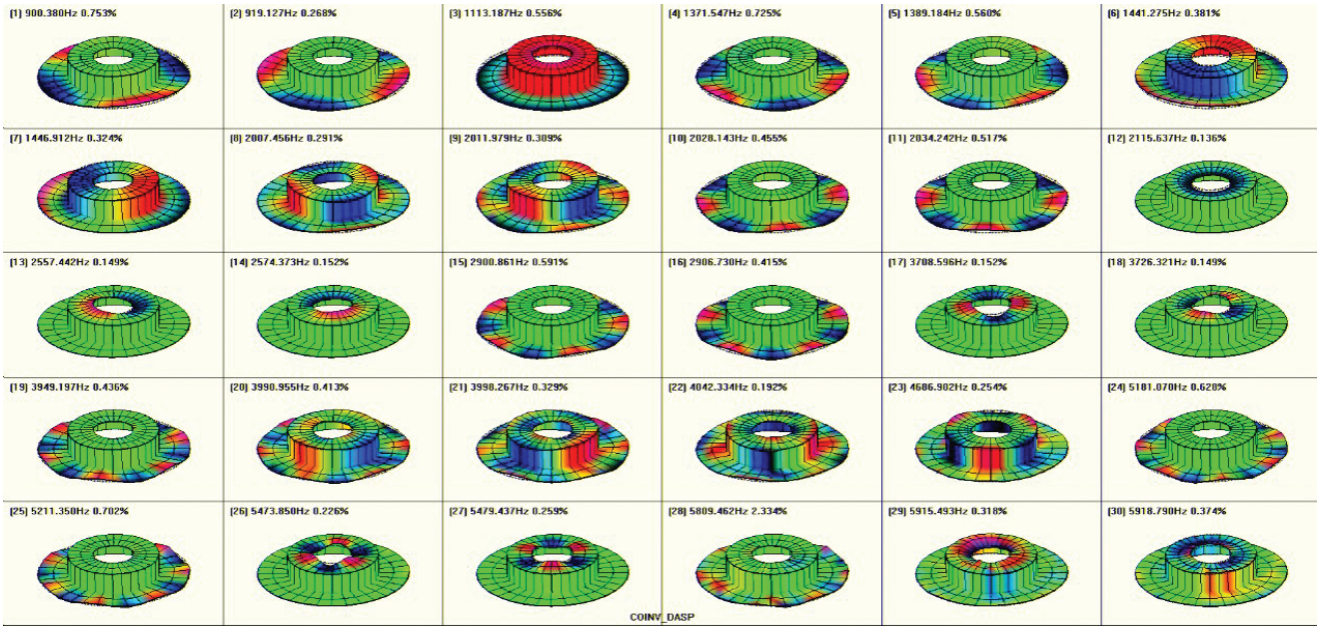


Fig. 5 Modal shapes optimized by algorithm 2

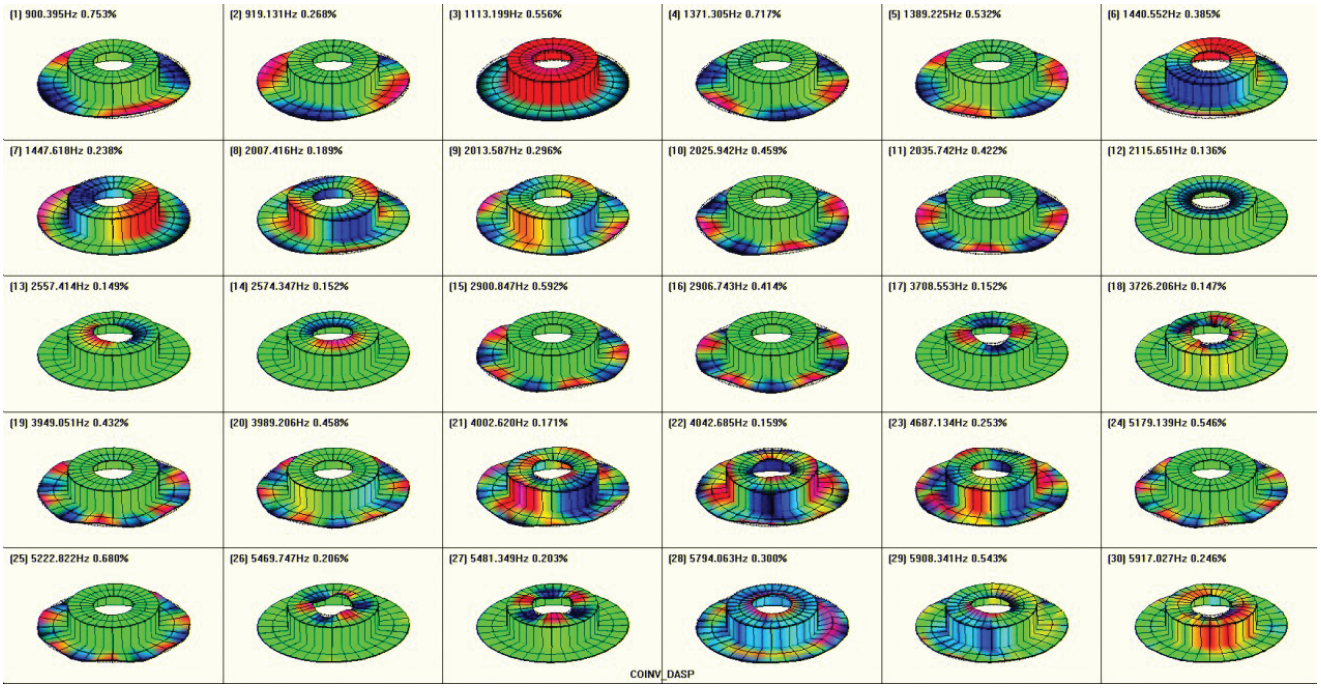


Fig. 6 Modal shapes optimized by algorithm 3

Discussion

Using the identified modal parameters as the initial solution and performing optimization can obtain the optimal solution that can best matches the synthesized FRF or half spectrum with the measured results in the least square sense. Optimization can unify the result of different parameter identification algorithms, and also can improve the accuracy of parameter identification. However, all modal frequencies, damping ratios, participators and modal shapes need to be optimized at the same time. If the number of measuring points and excitation points (EMA) or reference points (OMA) in MIMO test is large, extremely

Table 1 Fitting error comparison before and after optimization

Method	Initial Result		Algorithm 2		Proposed algorithm	
No.	Frequency(Hz)	Damping ratio(%)	Frequency(Hz)	Damping ratio(%)	Frequency(Hz)	Damping ratio(%)
1	900.218	0.273	900.380	0.753	900.395	0.753
2	918.849	0.559	919.127	0.268	919.131	0.268
3	1112.793	0.711	1113.187	0.556	1113.199	0.556
4	1371.190	0.535	1371.547	0.725	1371.305	0.716
5	1389.034	0.385	1389.184	0.560	1389.225	0.532
6	1440.139	0.246	1441.275	0.381	1440.552	0.384
7	1447.077	0.189	1446.912	0.324	1447.618	0.238
8	2006.526	0.192	2007.456	0.291	2007.416	0.189
9	2013.220	0.485	2011.979	0.309	2013.587	0.296
10	2025.731	0.429	2028.143	0.455	2025.942	0.459
11	2035.321	0.137	2034.242	0.517	2035.742	0.422
12	2114.900	0.152	2115.637	0.136	2115.651	0.136
13	2556.497	0.163	2557.442	0.149	2557.414	0.149
14	2573.301	0.578	2574.373	0.152	2574.347	0.152
15	2901.358	0.415	2900.861	0.591	2900.847	0.592
16	2906.301	0.158	2906.730	0.415	2906.743	0.414
17	3707.591	0.165	3708.596	0.152	3708.553	0.152
18	3725.080	0.463	3726.321	0.149	3726.206	0.147
19	3947.892	0.461	3949.197	0.435	3949.051	0.432
20	3989.068	0.222	3990.955	0.413	3989.206	0.457
21	4001.871	0.192	3998.267	0.329	4002.620	0.171
22	4042.755	0.197	4042.334	0.192	4042.685	0.159
23	4681.818	0.558	4686.902	0.254	4687.134	0.253
24	5178.906	0.647	5181.070	0.628	5179.139	0.547
25	5224.428	0.227	5211.350	0.702	5222.822	0.680
26	5468.604	0.208	5473.850	0.226	5469.747	0.206
27	5480.310	0.317	5479.437	0.259	5481.349	0.203
28	5797.055	0.506	5809.462	2.334	5794.063	0.300
29	5905.051	0.267	5915.493	0.318	5908.341	0.543
30	5915.970	0.655	5918.790	0.374	5917.027	0.246
31	6111.458	1.262	6258.083	2.836	6270.213	2.682
32	6164.628	0.273	6299.032	2.708	6292.603	2.790
Fitting error(%)	25.3953		16.3522		12.8469	

large-scale linear equations need to be solved in each loop of optimization, resulting in a long calculation time and making it impractical.

The optimization algorithm based on QR decomposition proposed in this paper first performs QR decomposition on the error data of each point separately, placing modal frequencies and damping ratios at the last part of the equation. Then all the data are combined into equation containing only modal frequency and damping ratio, the optimized modal frequencies and damping ratios are obtained using least squares method. Then, optimized participator can be solved with all curves of same excitation points or reference point, with similar QR decomposition method. The optimized modal shapes can be extract point by point with optimized poles and participators. The proposed optimization algorithm improves the optimization speed by hundreds or thousands of times for large number of measuring points in MIMO test with high orders, which make the optimization algorithm practical in engineering.

The feasibility of the new algorithm was verified with an engineering example, In the example of break disc modal test, the fitting error was reduced from 25.3953% to 12.8469%. All modal shapes after optimization are in accordance with the initial results.

References

1. Juang, J.-N., and Pappa, R.S. An Eigensystem Realization Algorithm for Modal Parameter Identification and Mode Reduction, Journal of Guidance, Control, and Dynamics, Vol 8, No. 1, 1985, pp 620-627

2. Allemang, R J, Brown, DL, and Fladung, W, Modal Parameter Estimation: A Unified Matrix Polynomial Approach, Proc. of the 12th IMAC,1994, pp. 501-514.
3. Bart Peeters, Patrick Guillaume, Herman Van der Auweraer, etc, Automotive and aerospace applications of the PolyMAX modal parameter estimation method. Proc. of 22th IMAC, 2004
4. J. M. Liu, S. W. Dong, M. Ying, S. Shen.Dynamic Parameters Identification Technology in Bridge Health Monitoring, Proceeding of the 14th ASIA PACIFIC VIBRATION CONFERENCE, 2011, Dec. HongKong
5. . van Overschee P, de Moor B. Subspace identification for linear systems: theory-implementation-applications[M]. Dordrecht, Netherlands: Kluwer Academic Publishers, 1996: 15−101.
6. B. PEETERS AND G. DE ROECK. Stochastic system identification for operational modal analysis: a review. ASME Journal of Dynamic Systems, Measurement, and Control, 123(4):659-667, 2001.
7. R.Brincker, L.Zhang, P.Andersen, Modal identification from ambient responses using frequency domain decomposition, Proceedings of the 18th IMAC, 2000
8. J. M. Liu, S. Shen, M. Ying and S. W. Dong, The Optimization and Autonomous Identification of Modal Parameters, Modal Analysis Topics, Volume 3,Conference Proceedings of the Society for Experimental Mechanics Series, 2011, Volume 6, 203-214.